REPORT DOCUMENTATION PAGE

Form Approved OMB NO. 0704-0188

1. REPORT DATE (DD-MM-YYYY)	2. REPORT TYPE	3. DATES COVERED (From - To)
	New Reprint	-

4. TITLE AND SUBTITLE
Strain-balanced InAs/InAs1-xSbx type-II superlattices grown by molecular beam epitaxy on GaSb substrates

5a. CONTRACT NUMBER
W911NF-10-1-0524

5b. GRANT NUMBER

5c. PROGRAM ELEMENT NUMBER
611103

6. AUTHORS
Kalyan Nunna, Elizabeth H. Steenbergen, Lu Ouyang, Bruno Ullrich, Diana L. Huffaker, David J. Smith, Yong-Hang Zhang

5d. PROJECT NUMBER

5e. TASK NUMBER

5f. WORK UNIT NUMBER

7. PERFORMING ORGANIZATION NAMES AND ADDRESSES
University of Illinois - Urbana
Board of Trustees of the University of Illinois
1901 S First Street
Champaign, IL 61820 -7473

8. PERFORMING ORGANIZATION REPORT NUMBER

9. SPONSORING/MONITORING AGENCY NAME(S) AND ADDRESS(ES)
U.S. Army Research Office
P.O. Box 12211
Research Triangle Park, NC 27709-2211

10. SPONSOR/MONITOR'S ACRONYM(S)
ARO

11. SPONSOR/MONITOR'S REPORT NUMBER(S)
58141-EL-MUR.12

12. DISTRIBUTION AVAILIBILITY STATEMENT
Approved for public release; distribution is unlimited.

13. SUPPLEMENTARY NOTES
The views, opinions and/or findings contained in this report are those of the author(s) and should not contrued as an official Department of the Army position, policy or decision, unless so designated by other documentation.

14. ABSTRACT
Strain-balanced InAs/InAs1?xSbx type-II superlattices (SLs) on GaSb substrates with 0.27???x??0.33 were grown by molecular beam epitaxy and demonstrated photoluminescence (PL) up to 11.1??m. The calculated SL bandgap energies agree with the PL peaks to within 5?meV for long-wavelength infrared samples (9.5, 9.9, and 11.1??m) and to within 9?meV for a mid-wavelength infrared sample (5.9??m). X-ray diffraction measurements reveal average SL mismatches of less than 0.2%, and the PL full-width-at-half-maximums increase with the mismatch,

15. SUBJECT TERMS
antimony alloys, energy gap, gallium alloys, III-V semiconductors, molecular beam epitaxial growth, photoluminescence, semiconductor superlattices, X-ray diffraction

16. SECURITY CLASSIFICATION OF:			17. LIMITATION OF ABSTRACT	15. NUMBER OF PAGES	19a. NAME OF RESPONSIBLE PERSON
a. REPORT	b. ABSTRACT	c. THIS PAGE			Shun Chuang
UU	UU	UU	UU		19b. TELEPHONE NUMBER: 217-721-3031

Report Title

Strain-balanced InAs/InAs1-xSbx type-II superlattices grown by molecular beam epitaxy on GaSb substrates

ABSTRACT

Strain-balanced InAs/InAs1?xSbx type-II superlattices (SLs) on GaSb substrates with 0.27???x??0.33 were grown by molecular beam epitaxy and demonstrated photoluminescence (PL) up to 11.1??m. The calculated SL bandgap energies agree with the PL peaks to within 5?meV for long-wavelength infrared samples (9.5, 9.9, and 11.1??m) and to within 9?meV for a mid-wavelength infrared sample (5.9??m). X-ray diffraction measurements reveal average SL mismatches of less than 0.2%, and the PL full-width-at-half-maximums increase with the mismatch, confirming the importance of strain-balancing for material quality.

REPORT DOCUMENTATION PAGE (SF298)
(Continuation Sheet)

Continuation for Block 13

ARO Report Number 58141.12-EL-MUR
Strain-balanced InAs/InAs1-xSbx type-II superla ...

Block 13: Supplementary Note

Approved for public release; distribution is unlimited.

JVSTB
JOURNAL OF VACUUM SCIENCE AND TECHNOLOGY B

Strain-balanced InAs/InAs1−xSbx type-II superlattices grown by molecular beam epitaxy on GaSb substrates

Elizabeth H. Steenbergen, Kalyan Nunna, Lu Ouyang, Bruno Ullrich, Diana L. Huffaker et al.

Citation: J. Vac. Sci. Technol. B **30**, 02B107 (2012); doi: 10.1116/1.3672028
View online: http://dx.doi.org/10.1116/1.3672028
View Table of Contents: http://avspublications.org/resource/1/JVTBD9/v30/i2
Published by the AVS: Science & Technology of Materials, Interfaces, and Processing

Related Articles

Formation and morphological evolution of InAs quantum dots grown by chemical beam epitaxy
J. Vac. Sci. Technol. B 30, 051207 (2012)

Growth of epitaxial oxides on silicon using atomic layer deposition: Crystallization and annealing of TiO2 on SrTiO3-buffered Si(001)
J. Vac. Sci. Technol. B 30, 04E111 (2012)

Indium and impurity incorporation in InGaN films on polar, nonpolar, and semipolar GaN orientations grown by ammonia molecular beam epitaxy
J. Vac. Sci. Technol. A 30, 041513 (2012)

Successful growth of Cu2Se-free CuGaSe2 by migration-enhanced epitaxy
J. Vac. Sci. Technol. B 30, 02B126 (2012)

Optimization of Ohmic metal contacts for advanced GaAs-based CMOS device
J. Vac. Sci. Technol. B 30, 02B123 (2012)

Additional information on J. Vac. Sci. Technol. B

Journal Homepage: http://avspublications.org/jvstb
Journal Information: http://avspublications.org/jvstb/about/about_the_journal
Top downloads: http://avspublications.org/jvstb/top_20_most_downloaded
Information for Authors: http://avspublications.org/jvstb/authors/information_for_contributors

ADVERTISEMENT

Strain-balanced InAs/InAs$_{1-x}$Sb$_x$ type-II superlattices grown by molecular beam epitaxy on GaSb substrates

Elizabeth H. Steenbergen
Center for Photonics Innovation and School of Electrical, Computer and Energy Engineering, Arizona State University, Tempe, Arizona 85287

Kalyan Nunna
California NanoSystems Institute, University of California, Los Angeles, California 90095

Lu Ouyang
Department of Physics, Arizona State University, Tempe, Arizona 85287

Bruno Ullrich
Air Force Research Lab, Materials & Manufacturing Directorate, Wright Patterson AFB, Ohio 45433-7707

Diana L. Huffaker
California NanoSystems Institute, University of California, Los Angeles, California 90095

David J. Smith
Department of Physics and Center for Photonics Innovation, Arizona State University, Tempe, Arizona 85287

Yong-Hang Zhang[a)]
Center for Photonics Innovation and School of Electrical, Computer and Energy Engineering, Arizona State University, Tempe, Arizona 85287

(Received 26 October 2011; accepted 3 December 2011; published 21 December 2011)

Strain-balanced InAs/InAs$_{1-x}$Sb$_x$ type-II superlattices (SLs) on GaSb substrates with $0.27 \leq x \leq 0.33$ were grown by molecular beam epitaxy and demonstrated photoluminescence (PL) up to 11.1 μm. The calculated SL bandgap energies agree with the PL peaks to within 5 meV for long-wavelength infrared samples (9.5, 9.9, and 11.1 μm) and to within 9 meV for a mid-wavelength infrared sample (5.9 μm). X-ray diffraction measurements reveal average SL mismatches of less than 0.2%, and the PL full-width-at-half-maximums increase with the mismatch, confirming the importance of strain-balancing for material quality. © *2012 American Vacuum Society*. [DOI: 10.1116/1.3672028]

I. INTRODUCTION

Antimonide-based type-II superlattices (T2SLs) have many potential advantages over bulk HgCdTe for infrared photodetector materials,[1] with the InAs/(In)GaSb T2SL being the most investigated. However, short minority carrier lifetimes[2,3] in InAs/(In)GaSb T2SLs are detrimental to the detector dark current and quantum efficiency[4] and have recently been partially attributed to acceptorlike defects in GaSb[2] rather than the interfaces.[5] With Ga being the suspected culprit of the short minority carrier lifetime, the Ga-free InAs/InAs$_{1-x}$Sb$_x$ T2SL has the potential for longer lifetimes. The "stabilized Fermi level" due to intrinsic point defects in bulk InAs is expected to be above the conduction band edge,[6] rendering any midgap defect states inactive for Shockley–Read-Hall (SRH) processes. In comparison, the stabilized Fermi level for bulk GaSb is expected to be in the bandgap near the valence band edge,[6] leaving the midgap states available for SRH recombination. Relatively high photoluminescence (PL) efficiencies for 4 – 11 μm emission from InAs/InAs$_{1-x}$Sb$_x$ T2SLs grown on GaAs with highly dislocated 1 μm InAsSb buffer layers also suggest that As-rich InAs$_{1-x}$Sb$_x$ alloys have comparatively low SRH recombination coefficients.[7] A minority carrier lifetime of 250 ns reported for bulk InAs$_{0.80}$Sb$_{0.20}$ having a PL peak at 5.4 μm at 77 K[2] further supports the possibility that the InAs/InAs$_{1-x}$Sb$_x$ T2SLs may have longer lifetimes than those of the InAs/(In)GaSb T2SLs. Theoretically calculated absorption of an 11 μm InAs/InAs$_{1-x}$Sb$_x$ T2SL was lower, but within a factor of two, than that of a 10 μm InAs/(In)GaSb T2SL.[8] The theoretical study did not include SRH recombination, leaving open the possibility that in practice, the former T2SL may have higher absorption and a longer minority carrier lifetime than the latter due to interface and growth-related variations.[8]

Although not as well studied as InAs/(In)GaSb T2SLs, InAs$_{1-x}$Sb$_x$/InAs$_{1-y}$Sb$_y$ T2SLs have been investigated by several groups since their first proposal, which proposed utilizing tensile strain to reach longer wavelengths than bulk InAs$_{1-x}$Sb$_x$, to possibly compete with HgCdTe.[9] InAs$_{1-x}$Sb$_x$/InAs$_{1-y}$Sb$_y$ SLs were grown by both molecular beam epitaxy (MBE) and metalorganic chemical vapor deposition (MOCVD) with complicated strain-relieving buffer layers: (1) on InSb for LWIR (8–12 μm) photodetectors,[10,11] (2) on InAs for MWIR lasers,[12–14] (3) on GaAs for LWIR LEDs,[7,15] and (4) on GaSb for LWIR photodetectors.[16–18] However, the growth of InAs/InAs$_{1-x}$Sb$_x$ T2SLs on GaSb by MBE has not yet been reported. This article reports the design, MBE growth, and characterization of a set of strain-balanced InAs/

[a)]Author to whom correspondence should be addressed; electronic mail: yhzhang@asu.edu

InAs$_{1-x}$Sb$_x$ T2SLs on GaSb substrates for MWIR and LWIR detectors.

II. MODELING

InAs/InAs$_{1-x}$Sb$_x$ T2SLs can be strain balanced on GaSb by choosing appropriate combinations of layer thicknesses and InAs$_{1-x}$Sb$_x$ alloy compositions. In order to achieve high quality materials with low misfit dislocation densities, the critical thicknesses[19] of InAs and InAs$_{1-x}$Sb$_x$ on GaSb are used as the limits for the layer thicknesses in the strain-balanced T2SL designs. The zero-stress method,[20] which takes the elastic constants of the layers into account, is used to calculate the strain-balanced layer thicknesses. A three-band envelope function approximation model,[21] which includes coupling between the electrons, light holes, and spin-orbit split-off holes, is used to calculate the T2SL effective bandgap defined as the electron to heavy hole transition energy. The InAs, InSb, and InAs$_{1-x}$Sb$_x$ parameters are taken from Ref. 22. Recent studies using the type-IIb (electron well in the binary layer) alignment have found the bowing of the InAs$_{1-x}$Sb$_x$ valence band to be between 60–70% of the bandgap bowing.[18,23,24] The calculations presented here use the type-IIb alignment with 65% of the InAs$_{1-x}$Sb$_x$ bandgap bowing attributed to the valence band.

Figure 1 displays the calculated T2SL bandgap versus the layer thicknesses for strain-balanced designs on GaSb for three different InAs$_{1-x}$Sb$_x$ compositions. Within this composition range ($x \sim 0.25$–0.38), the InAs/InAs$_{1-x}$Sb$_x$ T2SL is shown to cover the MWIR and LWIR ranges. For a given composition, thicker layers result in smaller bandgaps, and the overlap between the electron and heavy-hole wave functions decreases. However, as the absorption coefficient is proportional to the square of the wave function overlap (and the density of states), larger overlaps are desirable. To optimize the wave function overlap for a particular bandgap, as shown in Fig. 2, the layers should be thin with higher Sb compositions in the InAs$_{1-x}$Sb$_x$ layer. The wave function

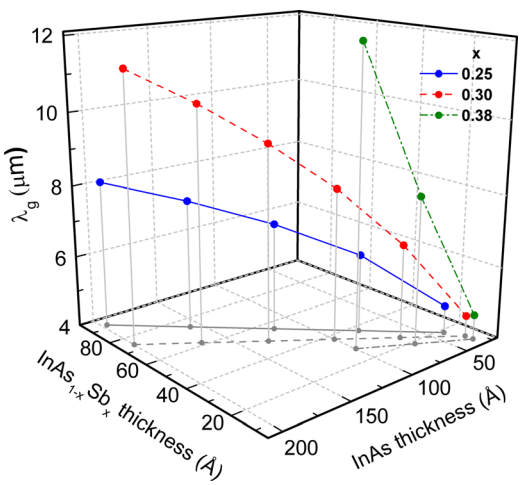

FIG. 1. (Color online) Calculated effective bandgaps for strain-balanced InAs/InAs$_{1-x}$Sb$_x$ type-II superlattices on GaSb substrates for three different Sb compositions.

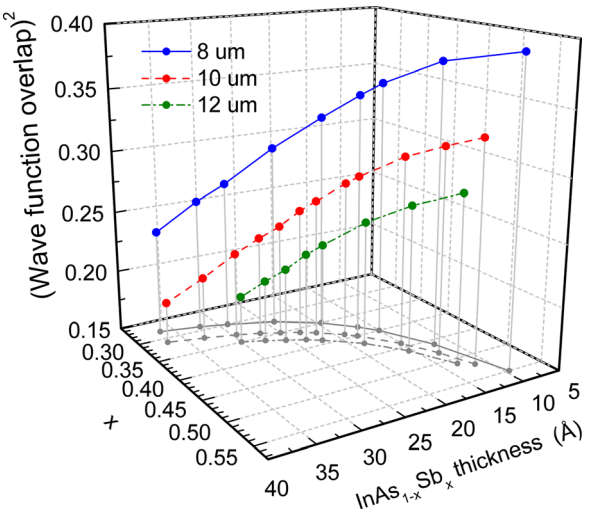

FIG. 2. (Color online) Calculated square of the electron-heavy-hole wave function overlap for different strain-balanced InAs/InAs$_{1-x}$Sb$_x$ type-II superlattice designs having bandgaps at 8, 10, and 12 μm.

overlap is inherently lower for the longer wavelength designs due to the higher Sb compositions resulting in larger valence band offsets and increased heavy-hole confinement.

III. EXPERIMENT

A. Molecular beam epitaxy growth

Several InAs/InAs$_{1-x}$Sb$_x$ T2SLs designs were grown on *n*-GaSb substrates by solid source MBE equipped with valved crackers set up to produce As_2 and Sb_2 species. Following the oxide desorption at 530 °C, a GaSb buffer layer was grown at 500 °C. The substrate was then cooled to 435 °C for the growth of the 500 nm InAs/InAs$_{1-x}$Sb$_x$ T2SL, and a final GaSb cap layer was grown at 480 °C. Four samples A, B, C, and D with 20 period SLs were grown under identical conditions with varying Sb/(As + Sb) beam equivalent pressure (BEP) flux ratios. The nonunity sticking coefficient of the group-V materials, As and Sb, and their competition for incorporation makes it difficult to control the group-V composition. However, by changing only the As flux and keeping all the remaining elements identical, a systematic variation in the Sb incorporation can be achieved. Thus, the InAs$_{1-x}$Sb$_x$ layers in samples A, B, C, and D have Sb/(As + Sb) BEP ratios of 0.32, 0.347, 0.378, and 0.412, respectively. Sample E consists of 60 T2SL periods with an overall thickness of 500 nm and 10 nm undoped AlSb barriers on either side of the overall T2SL to increase the PL intensity.

B. Characterization

The actual T2SL periods and InAs$_{1-x}$Sb$_x$ compositions were determined from the shutter times and the simulations of (004) ω-2θ coupled high-resolution XRD patterns recorded with a PANalytical X'Pert Pro MRD. The simulations use pseudomorphically strained layers on the GaSb substrate, which is reasonable given the results from a (224) reciprocal space map for sample B: only 0.2% relaxation and x differing by only 0.004 from the (004) ω-2θ scan value. Transmission

electron microscopy (TEM) characterization was carried out using a JEM-4000EX high-resolution electron microscope operated at 400 keV with a structural resolution of ~1.7 Å. The samples were prepared for observation along {110}-type zone-axis projections so that the direction of the electron beam would be aligned perpendicular to the growth surface normal. The PL measurements were carried out at 5 K using a continuous-wave 532 nm solid-state laser modulated at 60 kHz with an excitation intensity of 105 W/cm^2. The PL spectra were taken using a double-modulation technique with a Fourier transform infrared spectrometer to suppress the room temperature blackbody radiation.

IV. RESULTS AND DISCUSSION

A. X-ray diffraction

The (004) ω-2θ measurement and simulation results for the sample structure parameters are summarized in Table I, including the average T2SL mismatch with the substrate and the zero-order T2SL peak FWHM. The mismatch and FWHM for samples C and D are in italics to denote the zero-order T2SL peak position was calculated, due to its overlap with the substrate peak, based on the period and the T2SL satellite peak positions and that the FWHM is the mean of all the T2SL satellite peaks' FWHMs. Figure 3 shows the (004) ω-2θ profiles for samples B, C, and D. The relatively large T2SL period of 25 nm causes some envelope function modulation of the T2SL satellite peak intensities, reflecting the strain of the individual InAs and InAs$_{1-x}$Sb$_x$ layers, on the right and left of the substrate peak, respectively. These modulations result in the most intense T2SL peak no longer corresponding to the T2SL zero-order peak. The average T2SL mismatch in the growth direction is net tensile and less than 0.2% for all the samples, with sample D being the most closely lattice-matched to GaSb at 0.03%. Figure 4 shows the XRD data and simulation for sample E. The smaller T2SL period of sample E is evident from the greater T2SL satellite peak spacing.

B. Transmission electron microscopy

Cross-section electron micrographs of the different samples generally revealed well-defined SL layers and sharp interfaces, although some growth defects, mostly {111}-type stacking defects, were also visible in some places. The low-magnification TEM image of sample B, as shown in Fig. 5, reveals smooth interfaces and some defects, most starting at the substrate/buffer layer interface. A T2SL periodicity of 24.5 nm is measured, in very good agreement with the period from the XRD measurement. TEM images of sample A did not show evidence of dislocations, indicating the defect density is lower than that in sample B. Further details about TEM used to investigate the microstructure of InAs/InAs$_{1-x}$Sb$_x$ T2SLs with ordered and random InAs$_{1-x}$Sb$_x$ alloy layers grown by modulated and conventional MBE, respectively, are reported in a separate paper in this proceeding.[25]

TABLE I. Summary of the InAs/InAs$_{1-x}$Sb$_x$ T2SL structures.

Sample	x ±0.01	Period ±0.5 (nm)	Number of periods	XRD SL0 mismatch (ppm)	XRD SL0 peak FWHM (arcsec)
A (0203−1)	0.27	26.5	20	−1930	55
B (0218−1)	0.28	24.6	20	−1754	35
C (0218−2)	0.29	24.6	20	*−1164*	*39*
D (0218−3)	0.33	24.5	20	*−279*	*41*
E (0512−1)	0.30	7.4	60	−2231	92

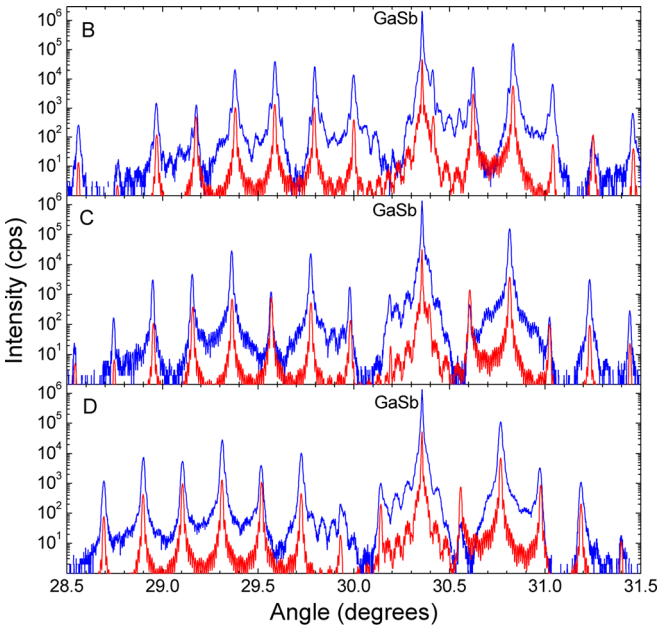

FIG. 3. (Color online) High-resolution ω-2θ x ray diffraction patterns and simulations (offset below the data) for the (004) reflection of InAs/InAs$_{1-x}$Sb$_x$ type-II superlattice samples B, C, and D.

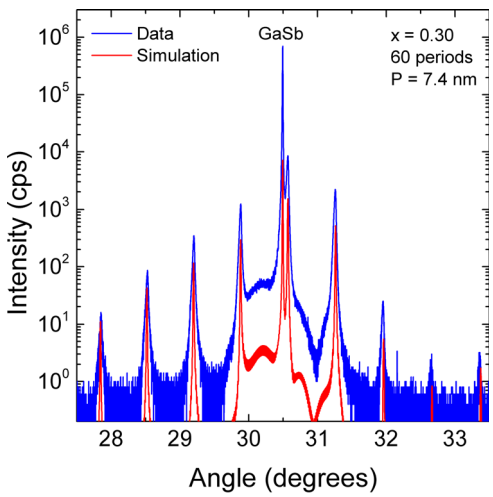

FIG. 4. (Color online) High-resolution ω-2θ x ray diffraction pattern and simulation (offset below the data) for the (004) reflection of sample E.

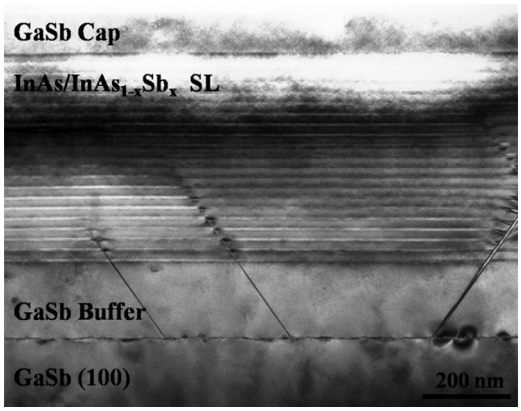

FIG. 5. Cross-sectional transmission electron micrograph showing typical defect microstructure of sample B which mostly consisted of {111}-type stacking faults originating at the GaSb (buffer)/GaSb substrate interface.

C. Photoluminescence

PL results for samples A, B, C, and E are shown in Fig. 6 with the symbols representing the data and the solid lines an eight-point adjacent-average smoothing of the data. Gaussian fits were applied, and the peak positions and FWHMs are shown in Table II. PL from sample D was not measurable. LWIR samples A, B, and C having similar periods confirm the expected trend of longer wavelength transitions for increasing Sb compositions. The PL intensity for sample B is approximately half that of samples A and C despite the similar emission wavelengths and wave function overlaps. This is presumably due to the greater number of dislocations originating at the substrate/buffer layer interface as shown in the TEM for sample B in Fig. 5. Sample E, with a significantly shorter period, results in MWIR emission that is more intense than the LWIR samples' emission due to the much higher wave function overlap and the AlSb electron barriers.

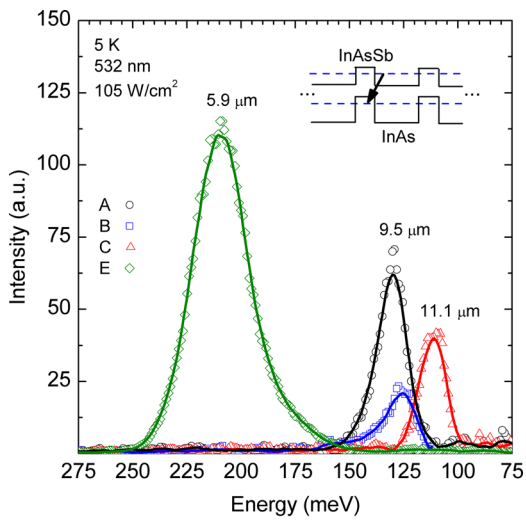

FIG. 6. (Color online) Photoluminescence spectra at 5 K for InAs/InAs$_{1-x}$Sb$_x$ type-II superlattice samples A, B, C, and E with varying compositions and periods. The data (symbols) are smoothed with eight-point adjacent-averaging (solid lines). The inset shows a schematic of the SL band alignment and PL transition.

TABLE II. Summary of the InAs/InAs$_{1-x}$Sb$_x$ T2SL calculated bandgaps and PL results.

Sample	Calculated bandgap at 0 K (meV/μm)	PL peak location at 5 K (meV/μm)	PL peak FWHM (meV)	Calculated $\left\|\int \Psi^*_{hh}\Psi_e dz\right\|^2$ (%)
A (0203−1)	128/9.7	130/9.5	18	6.1
B (0218−1)	120/10.4	125/9.9	17	7.0
C (0218−2)	107/11.6	112/11.1	14	6.6
D (0218−3)	72/17.1	—	—	5.6
E (0512−1)	218/5.7	209/5.9	33	45.2

The agreement between the calculated SL bandgaps and PL peaks is quite remarkable given the uncertainty in the material parameters and band offsets used in the calculation and in the measured Sb compositions and periods. The 14–18 meV FWHMs for samples A, B, and C correspond well with the 15–20 meV calculated bandgap shift results for a ± 0.01 change in x, whereas the layer thickness fluctuation barely affects the calculated bandgap due to the large SL period. Sample E, however, with a much smaller period and a 33 meV FWHM, experiences an approximately 30 meV bandgap shift for a ± 1 monolayer InAs$_{1-x}$Sb$_x$ thickness change but only $\sim$15 meV for ± 0.01 change in x. The PL peak FWHMs also follow the same tendency as the XRD average SL mismatch, a wider FWHM for a larger mismatch, demonstrating the correlation between strain-balancing and the SL material quality. Thus, strain-balancing is extremely important to avoid dislocations and achieve device quality SL materials.

V. SUMMARY AND CONCLUSIONS

In summary, strain-balanced InAs/InAs$_{1-x}$Sb$_x$ type-II SLs with $0.27 \leq x \leq 0.33$ were grown by molecular beam epitaxy and demonstrated photoluminescence spectra out to 11.1 μm, giving good agreement between the calculated SL bandgaps and photoluminescence peak positions. Transmission electron microscopy, along with x ray diffraction, and photoluminescence spectra line widths have shown the importance of strain-balancing to achieve high optical material quality with minimal dislocations. These findings indicate clearly that the InAs/InAs$_{1-x}$Sb$_x$ type-II SL is an excellent candidate for MWIR and LWIR device applications.

ACKNOWLEDGMENTS

This paper is based upon work supported in part by the U. S. Army Research Laboratory and the U. S. Army Research Office MURI program under Grant No. W911NF-10-1-0524 and Air Force Office of Scientific Research Grant No. (FA9550-10-1-0129). PL experiments were performed at AFRL/RXPS with the support of G. Brown. E.H.S. appreciates the DOD SMART and SFAz scholarships and

acknowledges the ASU Office of the Vice-President for Research and Economic Affairs, the Graduate Research Support Program, and the Graduate College.

[1]D. R. Rhiger, J. Electron. Mater. **40**, 1815 (2011).
[2]G. Belenky, G. Kipshidze, D. Donetsky, S. P. Svensson, W. L. Sarney, H. Hier, L. Shterengas, D. Wang, and Y. Lin, Proc. SPIE **8012**, 80120W (2011).
[3]B. C. Connelly, G. D. Metcalfe, H. Shen, and M. Wraback, Appl. Phys. Lett. **97**, 251117 (2010).
[4]S. Bandara, P. Maloney, N. Baril, J. Pellegrino, and M. Tidrow, Infrared Phys. Technol. **54**, 263 (2011).
[5]S. P. Svensson, D. Donetsky, D. Wang, P. Maloney, and G. Belenky, Proc. SPIE **7660**, 76601V (2010).
[6]W. Walukiewicz, Proc. Mat. Res. Soc. Symp. **148**, 137 (1989).
[7]P. J. P. Tang, M. J. Pullin, S. J. Chung, C. C. Phillips, R. A. Stradling, A. G. Norman, Y. B. Li, and L. Hart, Semicond. Sci. Technol. **10**, 1177 (1995).
[8]C. H. Grein, M. E. Flatte and H. Ehrenreich, in *Proceedings on the Third International Symposium on Long Wavelength Infrared Detectors and Arrays: Physics and Applications III*, Chicago, IL, 8–13 October 1995 (The Electrochemical Society, Inc., Pennington, NJ 1995), p. 211.
[9]G. C. Osbourn, J. Vac. Sci. Technol., B **2**, 176 (1984).
[10]S. R. Kurtz, L. R. Dawson, R. M. Biefeld, I. J. Fritz, and T. E. Zipperian, IEEE Electron Device Lett. **10**, 150 (1989).
[11]R. M. Biefeld, S. R. Kurtz, and S. A. Casalnuovo, J. Cryst. Growth **124**, 401 (1992).
[12]Y.-H. Zhang, "Mid-Wave Infrared InAs/InAsSb Type-II Superlattice Lasers" for "Strained Quantum Wells and their Applications," *Optoelectrical Properties of Semiconductor Quantum Wells and Superlattices* (Gorden and Breach, Amsterdam, The Netherlands, 1997).
[13]S. R. Kurtz, R. M. Biefeld, A. A. Allerman, A. J. Howard, M. H. Crawford, and M. W. Pelczynski, Appl. Phys. Lett. **68**, 1332 (1996).
[14]P. J. P. Tang, M. J. Pullin, Y. B. Li, C. C. Phillips, R. A. Stradling, S. J. Chung, W. T. Yuen, L. Hart, D. J. Bain, and I. Gaibraith, Appl. Phys. Lett. **69**, 2501 (1996).
[15]Y. B. Li, D. J. Bain, L. Hart, M. Livingstone, C. M. Ciesla, M. J. Pullin, P. J. P. Tang, W. T. Yuen, I. Galbraith, C. C. Phillips, C. R. Pidgeon and R. A. Stadling, Phys. Rev. B **55**, 4589 (1997).
[16]Y. Huang, J.-H. Ryou, R. D. Dupuis, V. R. D'Costa, E. H. Steenbergen, J. Fan, Y.-H. Zhang, A. Petschke, M. Mandl, and S.-L. Chuang, J. Cryst. Growth **314**, 92 (2011).
[17]S. R. Kurtz, L. R. Dawson, R. M. Biefeld, D. M. Follstaedt and B. L. Doyle, Phys. Rev. B **46**, 1909 (1992).
[18]D. Lackner, O. J. Pitts, M. Steger, A. Yang, M. L. W. Thewalt, and S. P. Watkins, Appl. Phys. Lett. **95**, 081906 (2009).
[19]J. W. Matthews and A. E. Blakeslee, J. Cryst. Growth **27**, 118 (1974).
[20]N. Ekins-Daukes, K. Kawaguchi, and J. Zhang, Cryst. Growth Des. **2**, 287 (2002).
[21]F. Szmulowicz, E. R. Heller, K. Fisher, and F. L. Madarasz, Superlattices Microstruct. **17**, 373 (1995).
[22]I. Vurgaftman, J. R. Meyer, and L. Ram-Mohan, J. Appl. Phys. **89**, 5815 (2001).
[23]P.-W. Liu, G. Tsai, H. H. Lin, A. Krier, Q. D. Zhuang, and M. Stone, Appl. Phys. Lett. **89**, 201115 (2006).
[24]C.-J. Wu, G. Tsai, and H.-H. Lin, Appl. Phys. Lett. **94**, 211906 (2009).
[25]L. Ouyang, E. H. Steenbergen, Y.-H. Zhang, K. Nunna, D. L. Huffaker, and D. J. Smith, "Structural properties of InAs/InAs$_{1-x}$Sbx type-II superlattices grown by molecular beam epitaxy," J. Vac, Sci. Technol. B (to be published).